Global Turbulence Simulations of CYCLONE Base Case and MAST Plasmas

S. Saarelma, R. Akers, M. Reshko, C.M. Roach, M. Romanelli, A. Thyagaraja and MAST team*, A. Peeters†, A. Bottino** and S. Jolliet‡

*EURATOM/UKAEA Fusion Association, Culham Science Centre, Abingdon, Oxfordshire OX143DB, United Kingdom
†Centre for Fusion, Space and Astrophysics, Warwick University, Coventry CV4 7AL, U.K.
**MPI für Plasmaphysik, EURATOM Association, D-85748 Garching, Germany
‡Centre de Recherches en Physique des Plasmas, Association EURATOM-Confédération Suisse, EPFL, 1015 Lausanne, Switzerland

Abstract. The non-local effects of turbulence can affect the transport especially in devices when the ration of ion gyroradius to plasma size (ρ_i*) is large. We show how the local linear and non-linear ITG flux-tube results are modified when the simulations are done with finite ρ_i* in a global code.

Keywords: gyrokinetic,turbulence
PACS: 52.30

INTRODUCTION

In tokamak plasmas the turbulence due to microinstabilites is known to be responsible for most of the cross-field transport of heat from the core of the plasma to the edge. The diffusivity associated with this "anomalous" transport is usually one order of magnitude larger than that of ion collisional transport. The frequencies of the observed micro-instabilities are much lower than the gyrofrequencies ($\Omega = Z_s eB/m_s$) of plasma particles s. This allows averaging particle motion over its gyro orbits leading to the gyrokinetic model of plasma instabilities.

The perpendicular wavelength of micro-instabilities are of the order of the gyroradius ($\rho_s = c_s/\Omega$, where c_s is the sound speed) of particles. Therefore, the gyromotion of particles have to be taken into account by gyroaveraging the fields within the particle orbit instead of using the value at the gyrocentre.

In this paper we use the gyrokinetic model to simulate turbulence in so called CYCLONE base case [1] and experimental MAST [2] plasmas with two codes: GS2 [3] that is a local flux-tube code and ORB5 [4, 5] that is a global code. The GS2 code is used to study sheared flow effects on linear stability and simulating non-linearly the microtearing modes. With ORB5 we investigate the global effect on ion temperature gradient (ITG) turbulence in a simple CYCLONE base case and then show the first results from non-linear simulations of MAST.

CP1069, *Theory of Fusion Plasmas, Joint Varenna-Lausanne International Workshop*
edited by X. Garbet, O. Sauter, and E. Sindoni

MAST PLASMAS AND THEIR SPECIAL EFFECTS ON GYROKINETIC SIMULATIONS

MAST is a spherical tokamak with achieved global parameters of $R \approx 0.85m$, $a \approx 0.5m$, $B_T < 0.52T$, $I_p < 1.4MA$. As can be seen from MAST plasma dimensions, a spherical tokamak has aspect ratio $A = R/a$ of the order of unity. The ratio of plasma pressure to the magnetic pressure $\beta = < p > /\mu_0 B^2$ is usually larger in spherical than in conventional large aspect ratio tokamaks. Due to the high NBI power to volume ratio and small radius plasma rotation speeds close to the ion sound speed can be achieved.

These properties specific to spherical tokamaks and MAST in particular affect the microinstabilities both linearly and non-linearly. The large variation of the toroidal magnetic field and the strong poloidal field that is comparable to the toroidal field enhance the ∇B drifts. The large trapped particle fraction $\sim \sqrt{1/A}$ can drive modes that combine the drive from temperature gradient and trapped electron drift precession frequency resonances. Large β means that the modes with magnetic perturbations become significant and they can not be ignored in the simulations. Electro magnetic modes such as microtearing mode can dominate the electro static modes especially at long wave lengths. On the other hand increasing β can have stabilising effect on toroidal drift modes [6]. The high β indicates also that for a relatively low magnetic field, MAST has a reasonably high temperature plasmas. Consequently, the ion gyroradius ρ_i is no longer small compared to the plasma radius a and the assumption that the equilibrium profiles to be constant in a simulation that spans several ρ_i in width is less valid.

The large rotation shear ω_{SE} can stabilize especially the long wave length ITG modes that have a relatively slow growth rate. The electron temperature gradient (ETG) modes are much less strongly affected by the flow shear.

FLUX TUBE GYROKINETIC SIMULATIONS OF MAST

We use GS2 gyrokinetic code for investigating the local microstability properties of MAST plasmas. GS2 is an initial value code that includes the full magnetic perturbation and collisions. It uses flux tube geometry that follows the field lines around the plasma from the outboard mid-plane to the inboard mid-plane. The code makes periodic copies of these flux tubes to make up the full annulus of the torus. The flux tube approximation assumes that the densities and temperatures and their gradient scale lengths are constant within the simulation domain. In GS2 x is the radial coordinate and y is the coordinate parallel to the flux surface but perpendicular to the magnetic field.

Equlibrium Flow Shear Effects on ITG Stability

Recently GS2 has been upgraded to handle sheared equilibrium $\mathbf{E} \times \mathbf{B}$ rotation [7]. The sheared rotation means that the radial mode number k_x changes during the simulation. In GS2 this is done so that the simulation is initialized with a range of k_x response matrices and the change in k_x is tracked and the nearest point approximation is used to

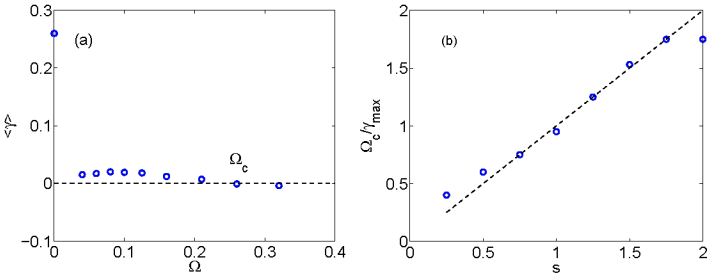

FIGURE 1. The linear growth rate as a function of rotation shear (a). Full stability is reached at when the growth rate becomes zero. This is marked with the critical rotation shear Ω_c. The critical rotation shear as a function of magnetic shear (b).

determine which matrix is used. Although this requires more computation in the initialization part, it is far cheaper than recalculating the implicit response matrices at every time step.

In a linear analysis we investigate a low-k_y mode stability as a function of rotation shear. We use the CYCLONE base case[1] equilibrium. The plasma shape is circular and the global physical parameters are B_T = 1.91T, a = 0.48m, R_0=1.32m, $T_e = T_i$. The local parameters at mid radius ($r/a = 0.5$) are q=1.42, R_0/L_T=6.9, L_n/L_T=3.12. We compare the maximum growth rate γ_{max} (no rotation shear) to the amount of rotation shear required to fully stabilize the mode, indicated by Ω_c in Fig. 1 (a).

When we vary the local magnetic shear we find that the ratio Ω_c/γ_{max} grows almost linearly with the shear as is shown in Fig 1 (b). The reason for this is that at high shear the resonant flux surfaces are closer to each other and the modes overlap more than at low shear. This makes it more difficult to tear the turbulent eddies apart by sheared rotation. The low magnetic shear in MAST core region combined with fast rotation can explain the low ion diffusivities observed in MAST [9].

Progress on Microtearing Simulations

GS2 calculations have found that microtearing modes, driven by the electron temperature gradient, are frequently linearly unstable at mid-radius in MAST plasma conditions [10]. Extensive gyrokinetic linear studies of microtearing mode properties [11] found the following: the primary microtearing mode drive is through the electron temperature gradient, but the growth rate is sensitive to magnetic drifts, collisionality, and β; the microtearing mode remained unstable even with an energy independent collision frequency, which would stabilise the mode in most analytic theories of microtearing; and an aspect ratio scan found that the microtearing mode drive reduced weakly with falling inverse aspect ratio r/R, and the instability remained for r/R as low as 0.1. The local aspect ratio of the typical ST flux surfaces where microtearing modes are unstable, is close to the aspect ratio of the edge region in conventional tokamaks.

It has been shown by a nonlinear model of microtearing turbulence that this could

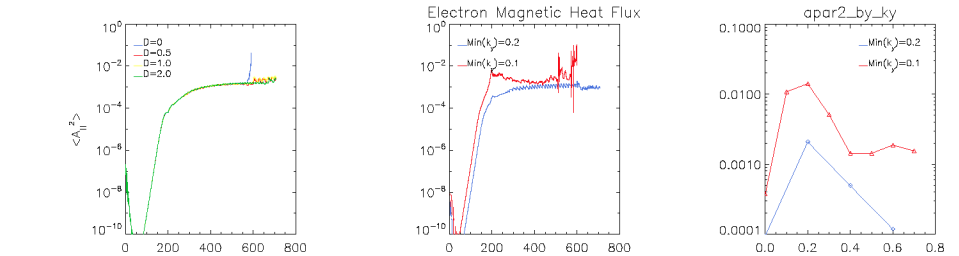

FIGURE 2. (a) Volume averaged amplitude of $A_\parallel^2$ versus time for nonliner microtearing simulations with different values of turbulent hyperviscosity D. (b) Electron parallel heat flux versus time for two nonlinear simulations resolving $k_y\rho_i = 0, 0.2, 0.4, 0.6$ (blue), and $k_y\rho_i = 0, 0.1, 0.2, 0.3, 0.4, 0.5, 0.6, 0.7$ (red). (c) $\langle A_\parallel (k_y)^2 \rangle$ at the final state for the simulation resolving 8 and 4 k_y modes (red and blue respectively).

be responsible for a substantial fraction of the electron heat flux in the region of NSTX plasmas where there is a significant electron temperature gradient [14]. Nonlinear gyrokinetic microtearing calculations are computationally demanding and have proved difficult [12, 13]. First simulations were carried out using an approximate s-α model fit to a MAST equilibrium, with some parameters tuned to reduce the parallel extent of the mode. Keeping only four perpendicular wavenumbers k_y (in the in-surface perpendicular direction), the turbulence started to saturate, but then the calculation became impractical owing to rapid growth at the highest radial wavenumbers k_x. An improvement to the GS2 collision operator [10] only transiently fixed the problem. The growth at high k_x is not believed to be physical, and could be arising from the accumulation of errors including those from the modelled collision operator.

More recent progress has been made by including a turbulent hyperviscosity damping term in the gyrokinetic equation:

$$\frac{\partial g_{k_x,k_y}}{\partial t} = -D\left(k_x^2 + k_y^2\right)^2 \sum_{k_x,k_y} |\phi_{k_x,k_y}|^2 \left(k_x^2 + k_y^2\right)^2 g_{k_x,k_y}$$

Including turbulent hyperviscosity had no impact on the linear physics, and suppressed rapid growth at high k_x later in the simulations. Furthermore, as shown in Figure 2(a) the turbulence saturation level was found to be insensitive to the numerical value of D. Having solved the problem at high k_x, the calculations proved to be sensitive with respect to resolution in k_y. Figures 2(b) and (c) show results from simulations with $k_y\rho_i = 0, 0.2, 0.4, 0.6$, and $k_y\rho_i = 0, 0.1, 0.2, 0.3, 0.4, 0.5, 0.6, 0.7$. The simulation that resolves lower k_y values finds significantly larger fluxes, and in both simulations the spectra show very large amplitudes in the lowest finite k_y that is resolved. It should be noted that for the approximate MAST parameters of this equilibrium, $k_y\rho_i = 0.1$ corresponds to a very low toroidal mode number $n \sim 4$. The magnetic shear in the simulation was artificially enhanced, and at low to moderate magnetic shear the large width in x of the required flux-tube may challenge the validity of the flux-tube approach.

GLOBAL GYROKINETIC SIMULATIONS

In MAST at mid radius $\rho_i > 10^{-2}a$. ITG modes have $k_\perp$ ranging from 0.1 to $1.0\rho_i$. Thus, the radial extent of the box for non-linear ITG flux tube simulations would become so large that the assumption that the equilibrium quantities and their gradient scale lengths are constant within the simulation region would be inaccurate. The only way to accurately simulate ITG turbulence in MAST is to use a global code that has a realistic equilibrium and models the profile variation within the simulation domain.

For global ITG simulations we have used the ORB5 code that uses the Particle-In-Cell (PIC) scheme for solving the gyrokinetic equation for the distribution function and combines this with a Poisson solver for the electric field. ORB5 uses the δf method, i.e. the distribution function is composed of equilibrium part that does not depend on the time and a perturbation that is time dependent, $f(\mathbf{R},t) = f_0(\mathbf{R}) + \delta f(\mathbf{R},t)$. In order to reduce noise ORB5 can use field-aligned filter that keeps only the modes with poloidal mode numbers $m = -nq(s) \pm \Delta m$, where n is the toroidal mode number, q is the safety factor and Δm is an input parameter. The filter is applied to the discretized perturbed density. The removed modes are not physically relevant since ITG modes tend to have $m \approx -nq$.

Linear Simulation for CYCLONE Base Case

First we compare linear GS2 flux tube code simulations with the global simulations using ORB5 for the CYCLONE test case. GS2 is run on a flux tube at mid radius and ORB5 is naturally a global simulation with radially varying profiles. We test the flux tube approximation by varying in the global simulation the $\rho* = \rho_i/a$ parameter as well as varying the width of the steep temperature gradient region. In ORB5 the temperature profile is parametrisized by formula:

$$\frac{1}{T}\frac{\partial T}{\partial \psi} = -\frac{a}{L_T}\frac{\cosh^{-2}\left(\frac{s-s_0}{\Delta}\right) - \cosh^{-2}\left(\frac{s_0}{\Delta}\right)}{1-\cosh^{-2}\left(\frac{s_0}{\Delta}\right)}. \quad (1)$$

Here L_T, Δ and s_0 are free parameters, ψ is the normalized poloidal flux and $s = \sqrt{\psi}$. In the width scan we keep all other parameters constant, but vary Δ. Therefore, the temperature and its gradient at mid radius (corresponds to $s_0 = 0.624$) stay constant. Figure 3 b) shows the profile variation with the Δ parameter. We compare the maximum linear growth rate from GS2 with the maximum linear growth rate of ORB5 which is affected by both $\rho*$ and the profile shape.

We use 40 million markers in ORB5 simulations and adjust the grid size according to $\rho*$ so that $N_s > 0.5/\rho*$, $N_\phi > 2/q(r = 0.5a)/\rho*$ and $N_\theta > 3/\rho*$. Here N_s, N_ϕ and N_θ are the number of radial, toroidal and poloidal grid points, respectively. We find that at small values of $\rho*$ the linear growth rates (normalized to v_{th}/a) of local and global codes agree within 10% of the growth rate, but as $\rho*$ gets large $> 1/50$, the results start to deviate from each other. This is shown in Fig. 3a). The reduction in growth rate for large values of $\rho*$ agrees with linear modelling by Garbet and Waltz [15] as well as Lin

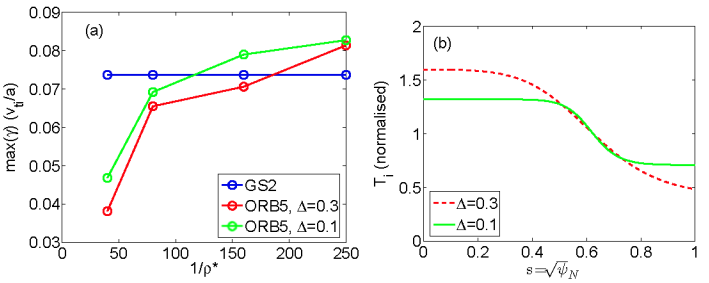

FIGURE 3. The linear growth rate of GS2 and ORB5 codes for CYCLONE test case as a function of $\rho*$ (a). The normalized temperature profiles as a function of $s = \sqrt{\psi_N}$ used in the simulations (b).

et al. [16]. On the other hand, the width of the gradient region has only weak effect on the normalized linear growth rate.

Non-Linear Simulation for CYCLONE Base Case

We have also run ORB5 in non-linear mode. Since there are no sources, the profiles relax due to the turbulence fluxes during the non-linear phase. The reduction in the gradient lowers the turbulence drive. Eventually the diffusivity decreases so much that the profile relaxation slows down and the simulation reaches a quasi steady state. At this point we stop the simulation and consider this the non-linear stability threshold. We vary $\rho*$ in the simulations and compare the relaxed normalized inverse temperature gradient length R_0/L_T (averaged around the steepest gradient region) at the threshold. As shown in Fig. 4, even though the linear growth rate showed a clear increasing trend with decreasing $\rho*$ the non-linear threshold is quite insensitive to the variation of $\rho*$. This result is similar to what has been obtained with the full-f code GYSELA [17].

The above simulations were done assuming an adiabatic response from the electrons, i.e. $\delta n_e/n_e = e\delta\phi/T_e$, where $\delta\phi$ is the perturbed electrostatic potential. Usually, this is reasonable assumption since the electron trajectories do not deviate far from the flux surfaces. However, treating electrons kinetically can affect the ITG mode stability [18, 19, 20]. We study the effect of trapped electrons with ORB5 by treating the passing particles with the adiabatic response but simulating the trapped electrons kinetically. The simulation was done in CYCLONE base case geometry with 512 million markers. The calculations were performed on HECToR supercomputer using 1024 processors for 120 hours. In Fig. 5 we show the time evolution of χ/χ_{GB} as a function of R_0/L_T. Here $\chi_{GB} = (\rho*)^2 c_s/a$ is the gyro-Bohm transport coefficient. The simulation starts at $R_0/L_T = 6.9$. At the end of the simulation the temperature gradients do not change any more, but have reached a steady state at $R_0/L_{T,i} \approx 4.7$ and $R_0/L_{T,e} \approx 5.5$. The steady state level of $R_0/L_{T,i}$ is significantly lower than the level obtained with the adiabatic electron response that was shown above to agree with the results in [1] (shown in Fig. 5 with a solid black line). This increased ITG turbulence in the non-linear phase due to the trapped electrons agrees with results in [18].

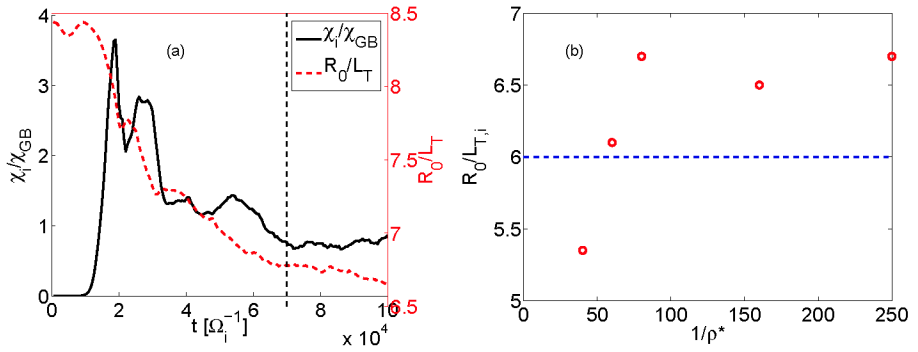

FIGURE 4. (a) The normalized diffusivity (χ/χ_{GB}) and inverse temperature gradient length (R_0/L_T) averaged over $0.55 < s < 0.7$ as a function of time in a non-linear ORB5 simulation with $\rho* = 1/500$. The vertical line shows the time when we determine the non-linear threshold. (b) The inverse temperature gradient length at the non-linear threshold as a function of $1/\rho*$. The horizontal line shows non-linear threshold value of R_0/L_T found in [1]

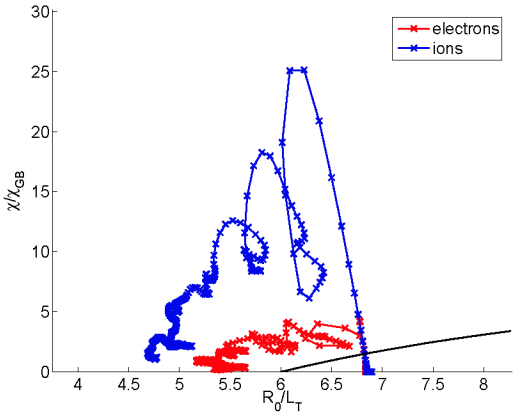

FIGURE 5. The normalized diffusivity (χ/χ_{GB}) as a function of inverse temperature gradient length (R_0/L_T) in a simulation with kinetic response for trapped electrons. The simulation starts at $R_0/L_T = 6.9$, χ/χ_{GB}=0. The solid line shows the non-linear stability limit for ITG with adiabatic electron response from [1].

ORB5 Simulations of MAST Plasmas

We use the equilibrium and plasma profiles of two well-diagnosed MAST discharges, one in L-mode (#12556 at 0.334s), one in H-mode (#13018 at 0.230s) in ORB5 simulation to determine the global linear and non-linear stability properties in the experiment. The global parameters of these discharges are identical, B_T=0.41T, I_p=730kA, P_{tot}=2MW. The experimental density and temperature profiles as well as the q-profile are shown in Fig. 6. The main difference in profiles is that the H-mode density profile is

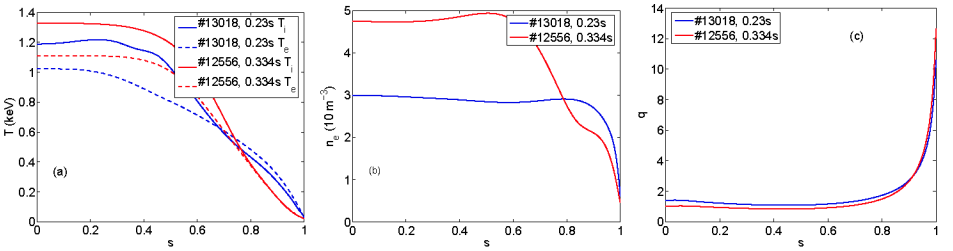

FIGURE 6. The radial (a) electron (dashed) and ion (solid) temperature, (b) electron density and (c) q-profiles of MAST H-mode (#13018 at 0.23s)) and L-mode (#12556 at 0.334s) discharges.

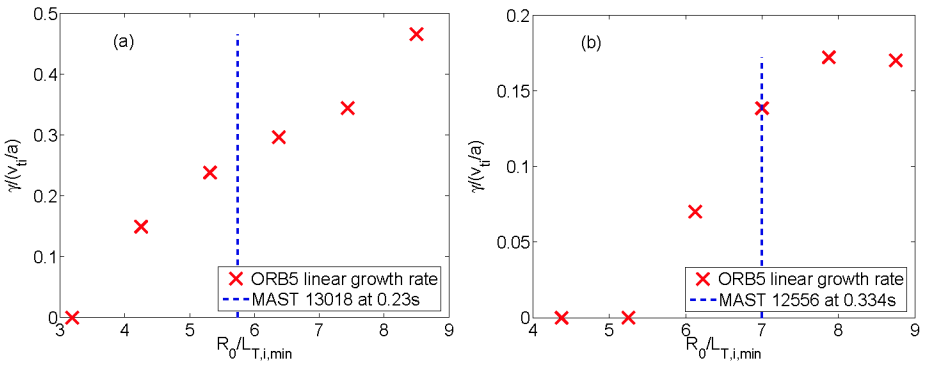

FIGURE 7. The linear growth rate of the fastest growing mode for (a) H-mode and (b) L-mode plasmas as a function of $R_0/L_{T,i}$. The vertical line represents the experimental value .

very flat except of the very edge. The steep gradient near the edge has little effect on the microstability in the gradient region ($s < 0.9$). Therefore, we ignore it in the simulation and assume that the density gradient vanishes at the edge to avoid numerical problems associated with steep gradients near the boundary of the simulation region. The temperature and q-profiles are quite similar with a slightly steeper temperature gradient in the L-mode. At the steepest gradient location $1/\rho* = 100$ in H-mode and 85 in L-mode.

We vary the steepness of the temperature gradient to determine the linear ITG stability limit for both plasmas. The runs are done in global geometry with adiabatic electron response using 40 million markers and recording the growth rate of the fastest growing mode. As shown in Fig. 7 both experimental plasmas are well within the unstable region. Radially the linear modes are localized in the region of $0.6 < s < 0.8$. This agrees with the earlier flux-tube results [10] where unstable ITG modes where found in this region of MAST plasmas.

We study the non-linear stability properties of the MAST plasmas by initializing the profiles slightly steeper than the actual experimental profiles and letting the turbulence develop and relax the profiles until we reach a steady-state. However the non-linear simulations for MAST plasmas using ORB5 are quite demanding because of the noise

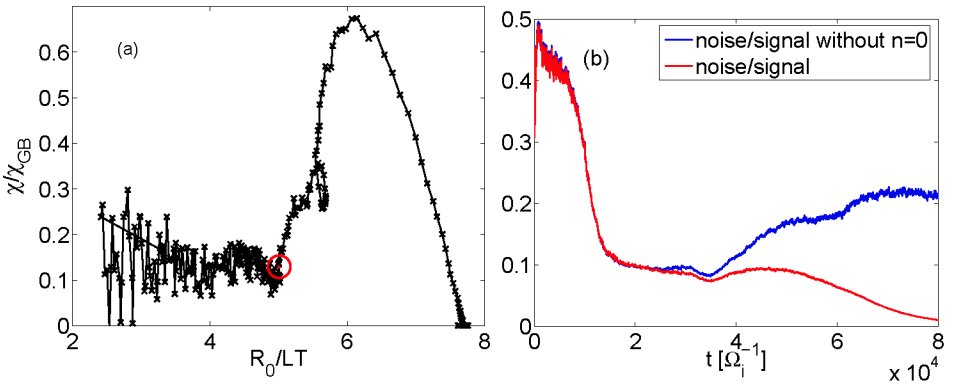

FIGURE 8. The diffusivity (χ/χ_{GB}) as a function of inverse temperature gradient length ($R_0/L_{T,i}$) averaged over $0.55 < s < 0.7$ for MAST H-mode plasma in ORB5 simulation (a) and the noise to signal ratio as a function of time (b). The red circle indicates the time $t = 40000\Omega^{-1}$ where the noise to signal without $n = 0$ ratio starts growing.

problem in the non-linear part of the simulation (we use 67 million markers). This can be seen in Fig. 8 where the normalized diffusivity is plotted as a function of $R_0/L_{T,i}$. After the initial growth the diffusivity decreases as the gradients relax. The turbulence reaches a plateau for a while at $\chi/\chi_{GB} = 0.1$, $R_0/L_{T,i} = 5$, but then the noise starts growing in the simulation and after that the results become unphysical.

We stop the simulation when the initial overshoot of the turbulent flux has disappeared, but the noise has not started growing and compare $\partial ln(1/T)/\partial s$ profiles around the mid-radius with the experimental MAST profiles at this point. As shown in Fig. 9 the ORB5 profiles are close to the MAST profiles, though sufficient simulation have not been performed to confirm this agreement is generally good. It must also be noted that in ORB5 simulations there are no sources. Nevertheless, the result indicates that the MAST temperature gradients are close to the non-linear stability threshold for ITG turbulence.

CONCLUSIONS AND DISCUSSION

Much has been learned about microstability and turbulence in spherical tokamak plasmas from local flux-tube simulations using the GS2 code [10]. Local flux-tube studies have identified the key linear instabilities, and have suggested that microtearing modes [11] should play an important role at mid-radius in MAST plasmas. Nonlinear local gyrokinetics simulations have also found that ETG turbulence can carry significant electron heat transport in MAST[21]. Equilibrium flow shear is also found to be comparable to the growth rates of ITG modes in MAST.

More recent advances in local gyrokinetic simulations with GS2 have included adding equilibrium $E \times B$ flow shear [7], and making progress with nonlinear microtearing simulations. Equilibrium flow shear calculations for the CYCLONE base case equilibrium

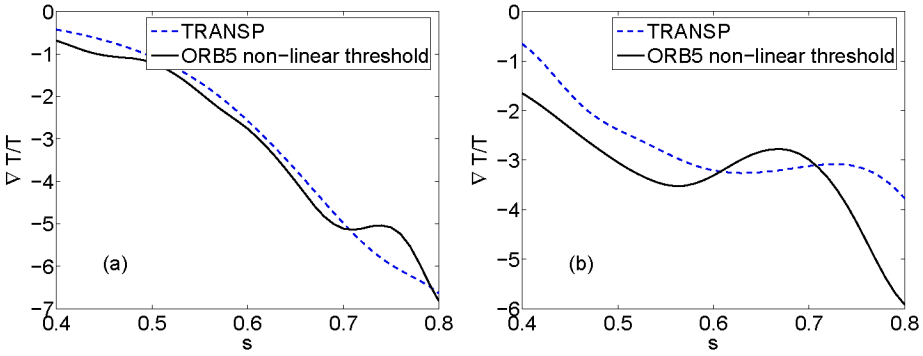

FIGURE 9. The radial $\partial ln(1/T)/\partial s$ profiles in MAST discharge (dashed) and at the non-linear stability threshold from ORB5 for L-mode (a) and H-mode (b) discharges.

with GS2 find that ITG modes become stabilised when the shearing rate becomes comparable to the growth rate, and it has also been found that the stabilising effect is sensitive to magnetic shear. Low magnetic shear makes the rotation shear more effective due to rational surfaces being radially further apart. Including turbulent hyperviscosity has permitted advances in nonlinear microtearing simulations. Turbulent hyperviscosity does not affect the linear and early nonlinear saturation phase, but selectively dissipates at high $k_\perp$ where unphysical growth had been responsible for polluted previous simulations. In these improved simulations it is now possible to assess convergence in other parameters, and at present we are finding that it is important to resolve low-k_y modes. Indeed for equilibrium parameters guided by those in MAST (but with enhanced magnetic shear and β in order to facilitate the simulations), it has been found necessary to resolve toroidal mode numbers n as low as 4.

Modelling nonlinear ITG turbulence (when these modes are unstable) in MAST requires global gyrokinetic simulations, as the local flux-tube approximation becomes inaccurate. We have therefore embarked on global gyrokinetic simulations with the global code ORB5.

Flux-tube result for linear ITG growth rates for the CYCLONE base case equilibrium has been reproduced using ORB5 with small $\rho*$. With large values of $\rho*$ the growth rate deviates from the flux-tube result, demonstrating the need for global simulations for plasmas in this regime.

Non-linear simulations (also for CYCLONE base case) show that while the linear growth rate depends on $\rho*$, the non-linear threshold is fairly insensitive to $\rho*$ variation. ORB5 simulations, including the kinetic response from trapped electrons, significantly increase the ITG turbulence compared to that found with a purely adiabatic electron response.

Global MAST simulations of H- and L-mode plasmas confirm the earlier flux-tube results that the MAST plasmas are linearly unstable for ITG modes (neglecting equilibrium flow shear). In the non-linear simulation the temperature gradients relax close to the experimental profiles showing that the MAST plasmas are close to the non-linear

threshold. Noise in the non-linear phase causes some problems interpreting the results. The future work will make use of the introduction of a Krook operator in ORB5 [22] that ensures that the marker weights do not grow too much and helps to reduce noise in the phase when the simulation approaches steady state. This should alleviate the noise problem in the future MAST simulations.

ACKNOWLEDGMENTS

This work was partly supported by the UK Engineering and Physical Sciences Research Council and by the European Communities under the contract of Association between EURATOM and UKAEA.. The views and opinions expressed herein do not necessarily reflect those of the European Commission. The ORB5 simulations with trapped electrons as well as non-linear MAST simulations required supercomputing resources that were made available by EPSRC during the early access period to HECToR.

REFERENCES

1. A M Dimits, G Bateman, M A Beer et al., Phys. Plasmas **7** (2000) 969.
2. B Lloyd et al. Nucl. Fusion **47** (2007) S658.
3. M Kotschenreuther, G Rewoldt and W M Tang Comput. Phys. Commun. **88** (1995) 128.
4. S Parker, C Kim and Y Chen, Phys. Plasmas **6** (1999) 1709.
5. S Jolliet, et al. Comput. Phys. Commun. **88** (1995) 128.
6. G Rewoldt, W M Tang, S Kaye and J Menard, Phys. Plasmas **3** (1996) 1667.
7. G W Hammett, W Dorland, N F Loureiro and T Tatsuno, Proceedings of the 48th APS Plasma Physics Division Meeting, Philadelphia (2006) VP1.00136.
8. M H Redi et al., 2003 Proc. 30th EPS Conf. on Controlled Fusion and Plasma Physics (St Petersburg) vol 27A (ECA) P-4.94.
9. R J Akers et al, Plasma Phys. Control. Fusion **45** (2003) A175-A204
10. C M Roach and D J Applegate and J W Connor and S C Cowley and W D Dorland and Hastie R J et al. Plasma Phys. Control. Fusion **47** (2005) B323.
11. D J Applegate et al, Plasma Phys. Contr. Fusion **49**, (2007) 1113.
12. D J Applegate, "Gyrokinetic Studies of a Spherical Tokamak H-mode Plasma", PhD thesis, Imperial College, London, (2007)
13. C M Roach et al, 14th European Physics Workshop, Greoux-les-Bains, France (2006)
14. K L Wong, S Kaye, D R Mikkelsen, J A Krommes, K Hill, R Bell and B LeBlanc, Physical Review Letters, **99** (2007) 135003.
15. X Garbet and R E Waltz, Phys. Plasmas **3** (1996) 1898.
16. Z Lin, S Ethier, T S Hahm, and W M Tang, Phys. Rev. Letters **88** (2002) 195004.
17. V Grandgirard et al. Plasma Phys. Control. Fusion **49** (2007) B173.
18. R D Sydora,, V K Decyk and J M Dawson, Plasma Phys. Control. Fusion **38** (1996) A281.
19. T Dannert and F Jenko, Phys Plasmas **12** (2005) 072309.
20. A Bottino, et al., Phys Plasmas **11** (2004) 198.
21. N Joiner et al. Plasma Phys. Control. Fusion **48** (2006) 685.
22. B F McMillan, S Jolliet, T M Tran, L Villard et al. Phys Plasma **15** (2008) 052308.